JPEDAV (2008) 29:231–238
DOI: 10.1007/s11669-008-9281-4
1547-7037 ©The Author(s)

Phase Diagram Mapping of the Fe_3Al-Cr-Mo-C Pseudo-Quaternary System at 800 °C Using a New Diffusion-Multiple Technique

Satoru Kobayashi and Stefan Zaefferer

(Submitted May 15, 2007; in revised form November 15, 2007)

A new diffusion-multiple technique was used for mapping the phase diagram in the pseudo-quaternary Fe_3Al-Cr-Mo-C system at 800 °C. The following five carbide phases were formed in an Fe_3Al matrix phase (B2) with composition gradients of Cr, Mo, and C in the diffusion-multiple samples: κ-Fe_3AlC, M_5C, M_6C, Cr_7C_3, and M_2C (M: Mo, Cr, Al, and Fe). It was assumed that B2 phase is in equilibrium with κ, M_5C, M_6C, and Cr_7C_3 but not with M_2C phase at 800 °C. Complex phase equilibria among those phases were efficiently mapped by the diffusion-multiple technique. The results from the technique were consistent with those obtained from the conventional bulk alloy method.

Keywords diffusion, EBSD, EDS, iron aluminide, precipitation

1. Introduction

A diffusion-multiple technique for the mapping of ternary phase diagrams was recently proposed by Zhao et al.[1,2] A diffusion-multiple is a dense assembly of three or more different metal pieces. This multiple is subjected to high temperatures to allow interdiffusion reactions along two-dimensional composition gradients. The interdiffusion among the elements forms all the intermetallic compounds and solid-solution phases in the ternary system defined the compositions of the assembly. Advanced microanalysis using electron backscatter diffraction (EBSD) for crystal structure analysis and energy dispersive x-ray spectroscopy (EDX) for quantitative composition analysis in the SEM makes diffusion-multiples a highly efficient approach for mapping phase diagrams.

The conventional method, in contrast, determines phase diagrams by using several bulk alloys. In this method bulk alloys are equilibrated through phase transformations, especially precipitation reactions that occur by decrease in temperature due to the reduction of solubility of a solute element. The phases formed after long heat treatment are analyzed to study phase equilibria. The disadvantage of this method is that significant experimental effort is required for the determination of multi-component phase diagrams.

Recently we proposed a new diffusion-multiple technique to map the A-rich portion of an A-B-C-D quaternary phase diagram by a combination of two-dimensional composition gradients introduced by the diffusion-multiple technique and precipitation reactions caused by annealing heat treatment.[3] In this technique three kinds of binary alloys (A-xB, A-yC, A-zD) are selected in such way that additional elements B, C, and D, respectively, are soluble in the A-rich α phase at a high temperature, T_1. These alloys are joined and heat-treated at T_1, to introduce two-dimensional composition gradients among the elements A-D in the α matrix phase. A subsequent heat treatment at a lower temperature (annealing), T_2, reduces the solubility of each element, which allows precipitation of all phases that are in equilibrium with the matrix phase (α) in that quaternary system. By analysis of microstructure around the sample interfaces and the triple junction after long annealing, it is possible to determine phase equilibria between the α phase and precipitate phases.

Fe_3Al-based alloys with A2/B2/$D0_3$ structures have potential for high temperature applications because of excellent high-temperature corrosion and oxidation resistance, lighter density than steels, and relatively low materials costs.[4,5] The disadvantages of this alloy are poor high temperature mechanical properties above 600 °C and poor room temperature toughness.[4] Recently we studied the Fe_3Al-Cr-Mo-C pseudo-quaternary system to explore the stability of fine carbide particles for improving creep resistance and toughness of Fe_3Al-based alloys.[6-8] In this article phase equilibria in the Fe_3Al rich portion of the pseudo-quaternary Fe_3Al-Cr-Mo-C system were determined using the proposed diffusion-multiple technique. Results were compared with those obtained from the conventional bulk alloy method.

2. Experimental Procedures

2.1 Diffusion-Multiple Experiments

Table 1 summarizes the three ternary alloys chosen as end members for the diffusion-multiple experiments based

Satoru Kobayashi, Osaka Center for Industrial Materials Research, Institute for Materials Research, Tohoku University, 1-1 Gakuen-cho Naka-ku Sakai, Osaka 599-8531, Japan; and **Stefan Zaefferer,** Department of Microstructure Physics and Metal Forming, Max Planck Institute Für Eisenforschung GmbH, Max-Planck-Str. 1, D-40237 Dusseldorf, Germany. Contact e-mail: kobayashi@imr.tohoku.ac.jp.

Table 1 The nominal compositions of the alloys used for the diffusion-multiple experiment

	Bulk alloy composition, at.%				
Designation	Fe	Al	Cr	Mo	C
5Cr	Bal.	26.0	5.0	…	…
10Mo	Bal.	27.0	…	10.0	…
2C	Bal.	27.0	…	…	2.0

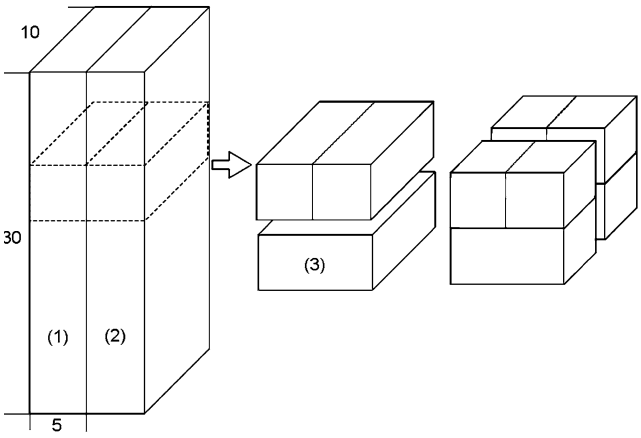

Fig. 1 Procedures to fabricate a diffusion-multiple sample

on literature reports concerning the ternary phase diagrams.[9-11] Hereafter the alloys are designated by 5Cr, 10Mo, and 2C, respectively. The matrix phase, B2, with approximate composition of Fe-(27-28)Al is regarded as one component. These alloys were prepared from 99.9% purity iron, 99.99% aluminium, 99.9% chromium, 99.9% molybdenum, and 99.9% carbon by induction melting in an argon atmosphere.

Since the diffusion of Mo and Cr is much slower than that of carbon, two pieces of 10Mo and 5Cr were first coupled. Pieces of $5\times10\times30$ mm^3 were cut from the ingot, coupled (see left in Fig. 1), and clamped between two austenitic stainless steel plates using ferritic stainless steel screws. The surfaces for welding were ground, mechanically polished, and electropolished with ethanol containing 8% perchloric acid under the conditions of 28 V, 10-15 °C for 20 s. This sample was heat-treated at 800 °C for 24 h for welding and at 1200 °C for 24 h for creating a long-range diffusion zone of Mo and Cr. Heat treatments were performed in a SiO_2 tube back filled with argon gas after evacuation to 6×10^{-4} Pa. This diffusion-couple was cut into pieces of $10\times10\times5$ mm^3 and then coupled with the piece of 2C (see center in Fig. 1), and heat-treated at 800 °C for 24 h and at 1200 °C for 15 min followed by water quenching. This coupled sample was cut into halves (see right in Fig. 1). It was confirmed in our previous paper[3] that the solute elements diffused well across the original interfaces. Subsequently the couples were heat treated at 800 °C for 300 h in the argon atmosphere. The surface was ground down by 500 μm and used for microstructure observation.

Table 2 The nominal compositions of the alloys used for the conventional bulk alloy method

	Nominal composition, at.%				
Alloy designation	Fe	Al	Cr	Mo	C
5-1.5-1	Bal.	25.4	5.0	1.5	1.0
2-1.5-0.6	Bal.	26.2	2.0	1.5	0.6
2-1.2-0.6	Bal.	26.0	2.0	1.2	0.6
0-1.2-0.6	Bal.	26.5	0	1.2	0.6
2-1-1.2	Bal.	25.9	2.0	1.0	1.2
0-1-1.2	Bal.	26.4	0	1.0	1.2

2.2 Conventional Bulk Alloy Experiments

Table 2 summarizes the alloy compositions used for the conventional bulk alloy experiments in this study. The melting procedure for these alloys was the same as the alloys for the diffusion-multiple experiment. Pieces of $10\times10\times15$ mm^3 were cut from the ingot and homogenized at 1200 °C in the α single-phase region for 15 min followed by water quench, and subsequently equilibrated at 800 °C for up to 1000 h followed by water quench. These heat treatments were performed in air. The samples were cut into halves and the cross sections were used for microstructure observations.

2.3 Phase Characterizations

Microstructure was examined by optical microscopy (OM) and high resolution scanning electron microscopy (HRSEM) equipped with a backscattered electron (BSE) detector, energy dispersive spectrometry (EDS), and EBSD camera. Phases present were identified by a combination of EDS and EBSD. For the EDS analyses, calibration curves were made to correlate the intensities of Fe, Al, Cr, and Mo with their compositions by using several as-cast alloys as standards with the assumption that the nominal compositions and the alloy compositions are equal. The carbon contents in carbide phases were determined by subtracting the compositions of the substitutional elements from 1: $x_C = 1-(x_{Fe} + x_{Al} + x_{Cr} + x_{Mo})$. Experimentally obtained EBSD patterns were fitted with simulated patterns of specific phases which we can expect based on compositional data by EDS. Simulated patterns were obtained by calculating structure factors for electron diffraction from the known atom positions in phases using the EDAX/TSL software Delphi and the computer program TOCA.[12,13] Table 3 lists six different phases identified in this study based on the structural and compositional analysis. Their crystal structures and compositional features are also summarized in Table 3. Examples of EBSD patterns experimentally obtained from the six phases and with the corresponding simulated patterns are shown in Fig. 2.

3. Results and Discussion

3.1 Phase Equilibria Obtained from the Diffusion-Multiple Experiments

Five types of carbide phases were formed in the Fe_3Al-based matrix with the composition gradient of Cr, Mo, and

C after the heat treatment at 800 °C for 300 h: κ-Fe_3AlC, M_5C, M_6C, Cr_7C_3, and M_2C (M: Mo, Cr, Al, and Fe). In our previous paper,[3] M_5C and M_6C phases were denoted by M_6C(H) and M_6C(L), respectively, since the crystal structure of these phases were not distinguished. It, however, turned out from more careful inspection of EBSD patterns that the crystal structures of these phases are different (see Table 3). Their notations were, therefore, changed. Figure 3 shows the chemical compositions of the carbide phases, plotted in an isothermal tetrahedron with the apices of (Fe-28Al), Cr, Mo, and C. Although all these phases are candidates for phases being in equilibrium with the B2 phase at 800 °C, microstructure must be carefully analyzed to determine which phases are in equilibrium with one another and which phases are just metastable precipitates.

Figure 4 shows an optical microstructure taken in the vicinity of the triple junction of the original interfaces in a diffusion-multiple sample heat treated at 800 °C for 300 h. The areas on which the five types of carbide phases were found in the B2 matrix are illustrated in this figure. It can be seen in the upper part of Fig. 4 that several types of carbide phases are formed and the types of the carbide phases change from Cr_7C_3, M_5C, and M_6C to M_2C when moving from the original 5Cr part into the 10Mo part. At the lower

Table 3 The phases identified in this study and their structural and compositional characteristics

Phase identified	Crystal structure	Typical composition, at.%
Matrix	B2 (ClCs, cP2 type)	Fe-(27-28)Al-(0-3)Cr-1Mo-C
κ-Fe_3AlC	$E2_1$ (CaO_3Ti, cP5 type)	Fe-22Al-(0-4)Cr-12C
Cr_7C_3	$D10_1$ (C_3Cr_7, oP40 type)	(45-50)Cr-(16-22)Fe-(2-3)Mo-30C
M_5C (a)	Orthorhombic symmetry	(44-47)Mo-14Fe-13Al-(5-10)Cr-18C
M_6C (b)	$E9_3$ (CFe_3W_3, cF112 type)	(44-47)Mo-23Fe-16Al-(0-3)Cr-14C
M_2C	$B8_1$ (NiAs, hP4 type)	(56-60)Mo-(12-15)Cr-4Fe-24C

(a) This phase is almost fitted to $D10_1$, but not exactly

(b) This phase can also be fitted to $NiTi_2$ (cF96) type. It is difficult to specify which phase is more accurate

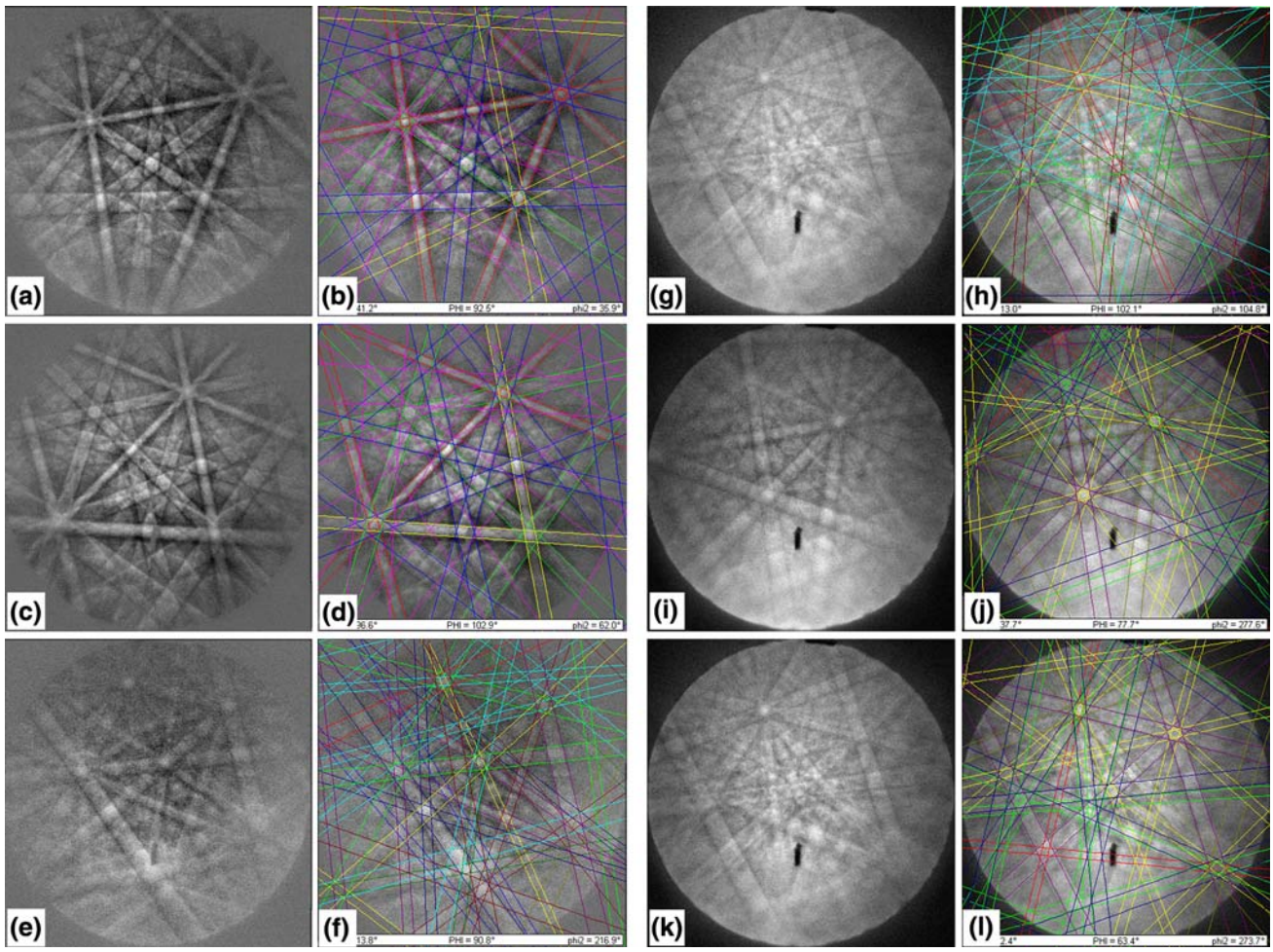

Fig. 2 Experimentally obtained EBSD patterns (a, c, e, g, i, and k) and the simulated patterns (b, d, f, h, j, and l) for (a, b) matrix (B2), (c, d) κ-Fe_3AlC ($E2_1$), (e, f) Cr_7C_3 ($D10_1$), (g, h) M_5C (orthorhombic), (i, j) M_6C ($E9_3$ or $NiTi_2$), and (k, l) M_2C ($B8_1$)

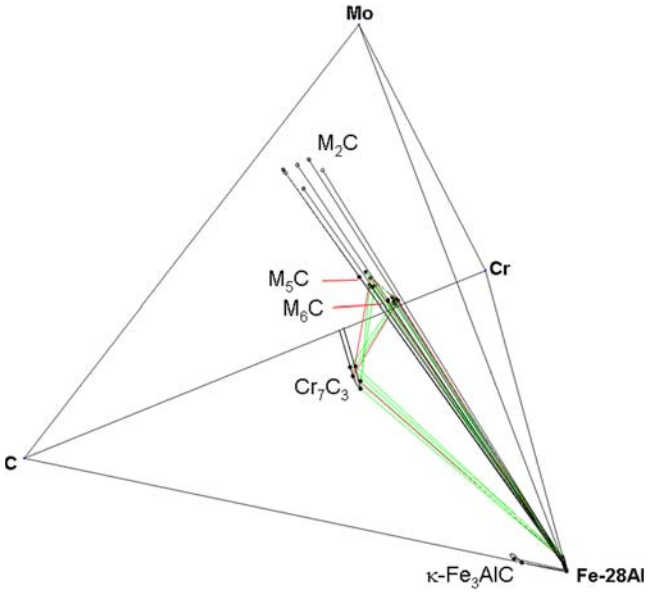

Fig. 3 The chemical compositions of the carbide phases appeared in a diffusion-multiple sample after the heat treatment at 800 °C for 300 h, plotted on the tetrahedron with apices of (Fe-28Al), Cr, Mo, and C

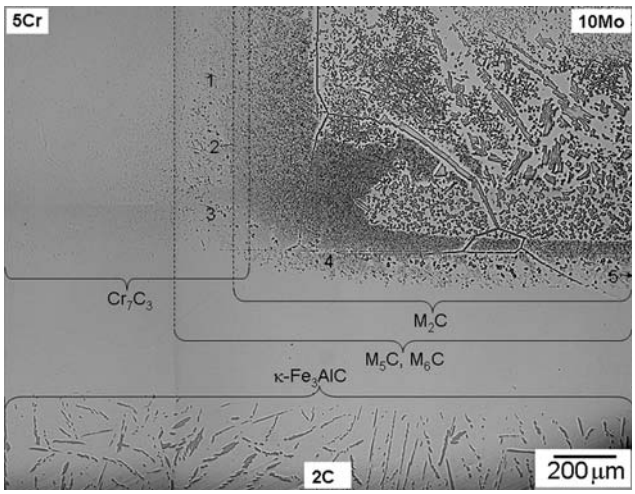

Fig. 4 Optical microstructure taken in the vicinity of the triple junction of a diffusion-multiple sample annealed at 800 °C for 300 h

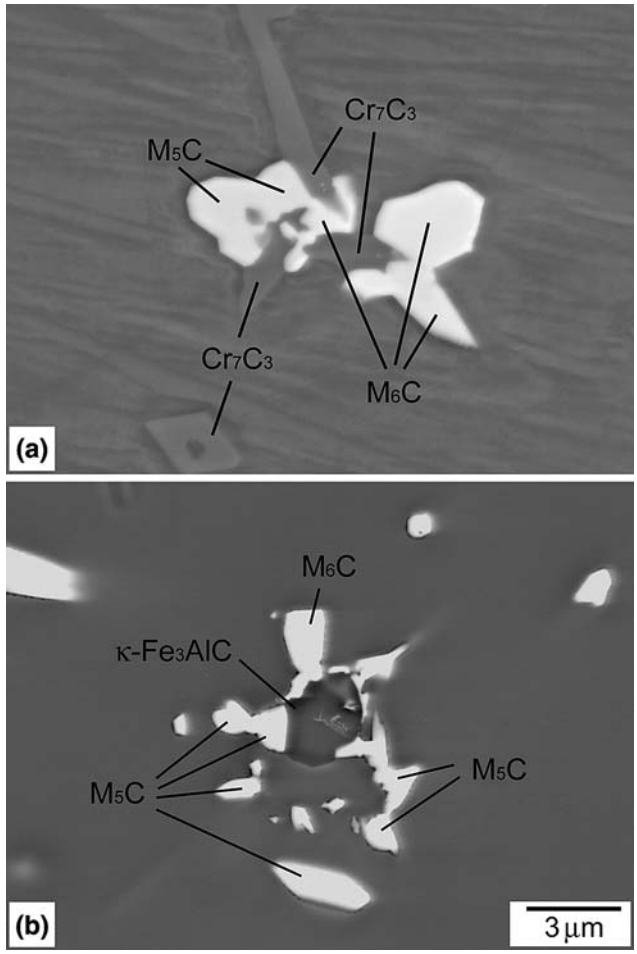

Fig. 5 Backscattered electron images taken from diffusion-multiple samples: (a) M_5C, M_6C, and Cr_7C_3 phases are formed in contact in the matrix in the area 2 in Fig. 4. Lines observed in the matrix are scratches from polishing. (b) M_5C, M_6C, and κ phases are formed in contact in a modified diffusion-multiple sample

part of Fig. 4 only κ-Fe_3AlC carbide needles can be seen below a carbide free layer.

Figure 5(a) shows a BSE image taken from area 2 in the upper part of Fig. 4. It can be observed that coarsened M_5C, M_6C, and Cr_7C_3 phases are formed in contact with each other. We can assume from this microstructure that a four-phase equilibrium region of $M_5C + M_6C + Cr_7C_3 + B2$ exists in this system. This microstructure was found in the limited area between area 1 at which M_6C and Cr_7C_3 phases are formed in contact in the matrix and area 3 at which M_5C and Cr_7C_3 phases are formed in contact. Table 4 summarizes the analyzed compositions of the phases that are formed in contact with each other in the different areas. It can be seen from the data for areas 1-5 in Table 4 that the M_6C phase was observed in the Cr-rich and Cr-poor matrix but the M_5C phase in between.

Our EDS analyses revealed that Cr and Mo do not exist in the carbide free layer and the area at which κ carbide is formed in the lower part of Fig. 4. The absence of Cr and Mo in the areas makes it impossible to determine phase relationship between κ phase and the other phases in our diffusion-multiple method. Diffusion paths along lines through the upper and lower parts in the 5Cr/2C part and 10Mo/2C part before and after annealing at 800 °C for 300 h are drawn on the isothermal sections of (Fe-27Al)-Cr-C and (Fe-27Al)-Mo-C system, respectively, and shown in Fig. 6. The diffusion paths show z-shaped curves in all the cases, passing through the α single phase region, and the

Table 4 The phases and their compositions obtained from the diffusion-multiple sample annealed at 800 °C for 300 h

		Phase composition, at.%				
Area analyzed	**Phase present**	**Fe**	**Al**	**Cr**	**Mo**	**C**
1	M_6C	22.3	16.0	3.5	43.9	14.3
	Cr_7C_3	14.1	1.0	52.1	2.7	30.1
	Matrix	69.0	27.2	2.9	0.9	…
2	M_5C	14.5	13.6	9.7	45.0	17.2
	M_6C	22.1	16.4	3.3	45.0	13.2
	Cr_7C_3	16.3	1.0	50.5	2.2	30.0
	Matrix	68.6	27.9	2.6	0.9	…
3	M_5C	14.4	14.2	9.8	44.2	17.4
	Cr_7C_3	19.3	0.9	47.1	2.8	29.9
	Matrix	68.7	28.1	2.4	0.8	…
4	M_5C	16.4	12.4	5.2	47.2	18.8
	M_6C	22.3	16.0	1.6	46.0	13.8
	Matrix	70.4	27.8	1.0	0.8	…
5	M_6C	22.8	15.9	0	47.2	14.1
	Matrix	71.2	28.0	0	0.8	…
6	M_5C	18.2	12.9	2.3	50.0	16.6
	M_6C	23.0	15.3	0.7	46.2	14.8
	κ-Fe_3AlC	63.3	22.1	0.9	0.3	13.4
	Matrix	70.8	28.0	0.9	0.3	…
7	Cr_7C_3	23.8	0.8	46.0	1.0	28.4
	κ-Fe_3AlC	61.0	20.9	3.4	0.1	14.6
	Matrix	70.2	28.0	1.5	0.3	…

The areas 1-5 correspond to those marked in Fig. 4. The areas 6 and 7 come from a modified sample. The EDS analysis is not precise enough to detect the carbon concentration in the matrix phase

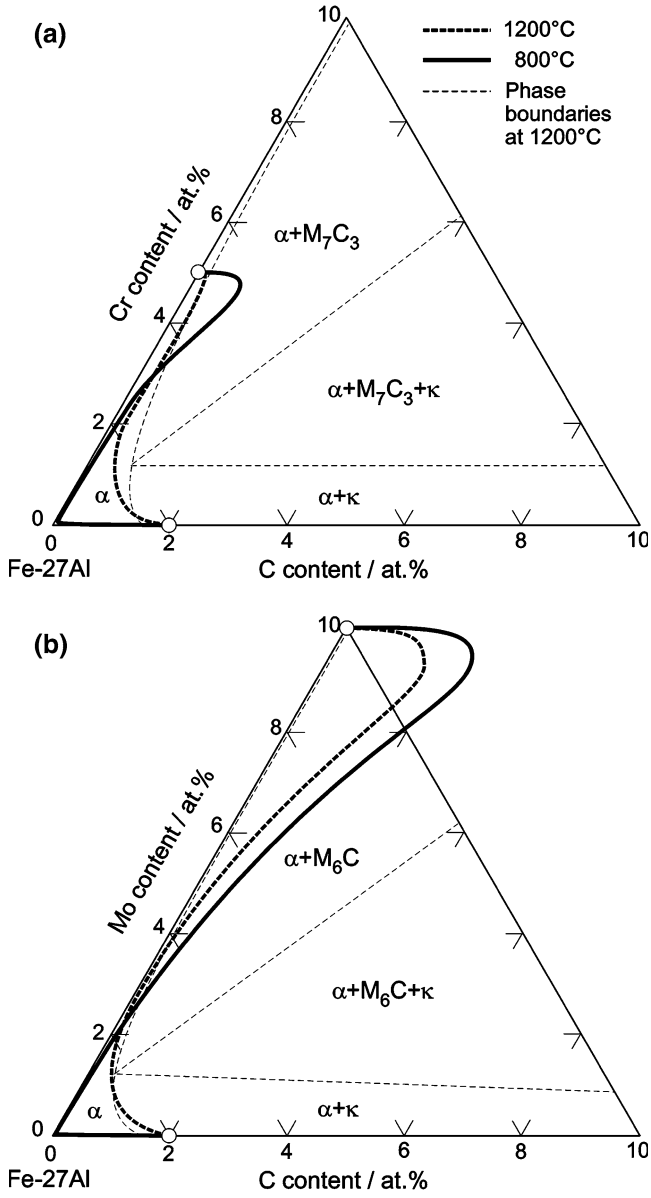

Fig. 6 Diffusion paths obtained from lines through the upper and lower parts in the (a) 5Cr/2C part and the (b) 10Mo/2Cr part before and after annealing at 800 °C for 300 h. Phase boundaries information at 1200 °C is also included in this figure. The solubility of C at 800 °C is extremely low and not drawn

z-shaped curves become enhanced after annealing at 800 °C. The z-shaped diffusion paths are formed presumably because C diffuses into the upper parts much quicker than Cr and Mo into the lower part. One cannot, therefore, avoid the enhancement of the z-shaped diffusion path by annealing as far as the upper part and the lower part are in contact with each other.

The following experiment was, then, newly performed; the original interface between the upper part and the lower part was mechanically cut before annealing at 800 °C to prevent C diffusion from the lower part into the upper part. In this modified sample κ phase was observed in the Cr and Mo containing matrix. Figure 5(b) shows a κ carbide particle formed in contact with M_5C and M_6C phases in the B2 matrix. The phase compositions obtained from these carbide phases formed in contact are listed as data 6 and 7 in Table 4.

The M_2C carbide phase, in contrast, formed very finely and rarely in contact with the other carbide phases even after coarsening, as shown in Fig. 7. Along grain boundaries this carbide was not observed and was replaced by coarse M_5C phase.[3] These observations suggest that the M_2C phase was precipitated as a metastable phase and not in equilibrium with the B2 matrix phase at 800 °C. We also found that the tie-lines between the M_2C phase and the matrix phase go through the four-phase tetrahedron of $M_5C + M_6C + Cr_7C_3 + B2$. This result supports the conclusion that M_2C is not thermodynamically stable within the B2 matrix at this temperature.

Based on the results obtained from the diffusion-multiple experiments, phase equilibria at 800 °C in the (Fe_3Al)-Cr-Mo-C system are discussed. Figure 8(a) and (b) displays the phase equilibria found in the system. In the composition range of high (Mo + Cr)/C ratios, the four-phase region of $M_5C + M_6C + Cr_7C_3 + B2$ exists (Fig. 8a). In the Cr-rich

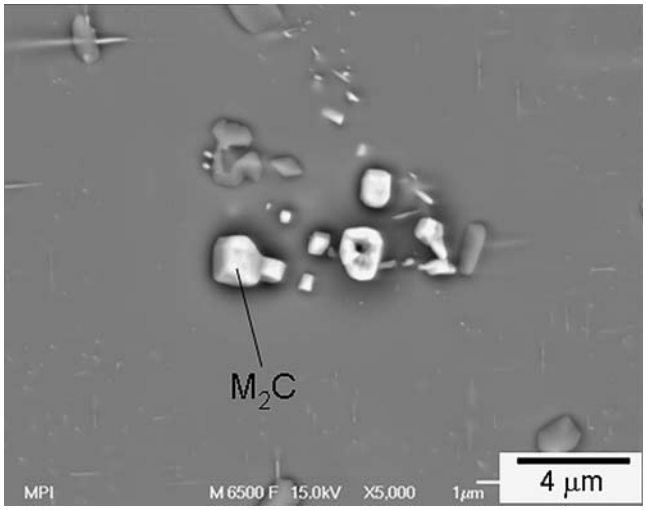

Fig. 7 Backscattered electron image taken in the vicinity of the triple junction in Fig. 4: coarse M_2C particles are formed in the matrix not in contact with other carbide phases

and Cr-poor sides, $M_6C + Cr_7C_3 + B2$ and $M_5C + Cr_7C_3 + B2$ three-phase region exists, respectively. It may be recognized that the Cr-poor M_6C phase is thermodynamically stable on the Cr-rich side and the Cr-rich M_5C on the Cr-poor side, which is seemingly inconsistent. This result can, however, be explained by the fact that the apex of the chemical composition of M_6C phase is located on the Cr-rich side of the four-phase tetrahedron (see Fig. 8a). In the composition range of low (Mo + Cr)/C ratios, the four-phase coexisting region of $M_5C + M_6C + \kappa\text{-}Fe_3AlC + B2$ and the three-phase region of $\kappa\text{-}Fe_3AlC + Cr_7C_3 + B2$ were found to exist, as drawn in Fig. 8(b). Taking the phase rules into account, it is reasonable to consider that the four-phase region of $M_5C + Cr_7C_3 + \kappa\text{-}Fe_3AlC + B2$ exists between these phase regions.

3.2 Reliability of the Results Obtained by the Diffusion-Multiple Technique

Results from the diffusion-multiple technique were compared with those obtained from the conventional bulk alloy method. The phases assumed as thermodynamically stable in the bulk alloys and their analyzed compositions are summarized in Table 5. The phase regions which we indicated are drawn in Fig. 8(c) and (d). Two types of three-phase coexisting region of $M_6C + Cr_7C_3 + B2$ (thinner triangle in Fig. 8c) and $M_5C + Cr_7C_3 + B2$ (thicker triangle in Fig. 8c) were found from the 5-1.5-1 and 2-1.2-0.6 alloys containing high and low Cr content, respectively. These results are reasonable in comparison with the existence and composition range of the $M_5C + M_6C + Cr_7C_3 + B2$ four-phase region which was found in the diffusion-multiple experiments. It can be seen from Table 5 that as the Cr content decreases in the matrix phase, M_6C carbide disappears and reappears together with M_5C or κ phase. This result is also consistent with the change in phase region with decreasing Cr content: $M_6C + Cr_7C_3 + B2 \rightarrow M_5C + M_6C + Cr_7C_3 + B2 \rightarrow M_5C + Cr_7C_3 + B2 \rightarrow M_5C + M_6C + \kappa\text{-}Fe_3AlC + B2$, which was indicated by the diffusion-multiple results. The four-phase coexisting region of $M_5C + Cr_7C_3 + \kappa\text{-}Fe_3AlC + B2$ was directly obtained from the alloy 2-1-1.2 (see Fig. 8d), with the assumption of validity of the diffusion-multiple data. Based on the comparisons above, it can be concluded that the results obtained from the two methods are consistent with each other and that the diffusion-multiple technique gives us as reliable data as the conventional method in determining phase equilibria.

3.3 The Efficiency of the Diffusion-Multiple Technique

In this study, the diffusion-multiple technique shows its effectiveness especially when many phase regions exist within a narrow composition range. In the Fe_3Al-Cr-Mo-C system, five phase regions exist within the composition range of 0-3 at.% Cr: $M_6C + Cr_7C_3 + B2$, $M_5C + M_6C + Cr_7C_3 + B2$, $M_5C + M_6C + B2$, $M_5C + M_6C + \kappa\text{-}Fe_3AlC + B2$, and $M_6C + \kappa\text{-}Fe_3AlC + B2$. One can imagine that many bulk alloys are necessary to obtain this knowledge using the conventional method. Even when many bulk alloys were prepared, those alloys might not hit the narrow composition ranges and thereby overlook the phase equilibria. In fact only three phase regions ($M_6C + Cr_7C_3 + B2$, $M_5C + M_6C + B2$, and $M_6C + \kappa\text{-}Fe_3AlC + B2$) were detected among the five regions by four bulk alloys (5-1.5-1, 2-1.5-0.6, 0-1.2-0.6, and 0-1-1.2) in this study (see Table 5), and it was difficult to deduce the transition of phase regions.

The diffusion-multiple technique can be a high efficiency approach for mapping phase diagrams if all the equilibrium phases were covered in a diffusion-multiple sample. To form equilibrium phases, a certain 'long' annealing time is needed. Too long annealing will, however, lose the areas in which the composition gradients of all the additional elements (Cr, Mo, and C in the case of this study) are overlapped with each other in the matrix. This area is called 'gradient overlapped area' below. It is, therefore, needed to find an optimized annealing time that depends on the elements included in the system under study. When the system contains solute elements of which the diffusion coefficients are much different like in this study, it was found that a special treatment was necessary to keep the gradient overlapped areas of C, Cr, and Mo. Preparing a few bulk alloys would help to confirm whether the results cover phase equilibria among all the phases in the system. In the systems that contain only solute elements of which the diffusion coefficients are similar, one can expect that it is easier to keep gradient overlapped areas, and this expectation is under investigation.

4. Conclusion

The diffusion-multiple technique was used to determine phase equilibria at 800 °C in the pseudo-quaternary Fe_3Al-Cr-Mo-C system. The results obtained from the technique

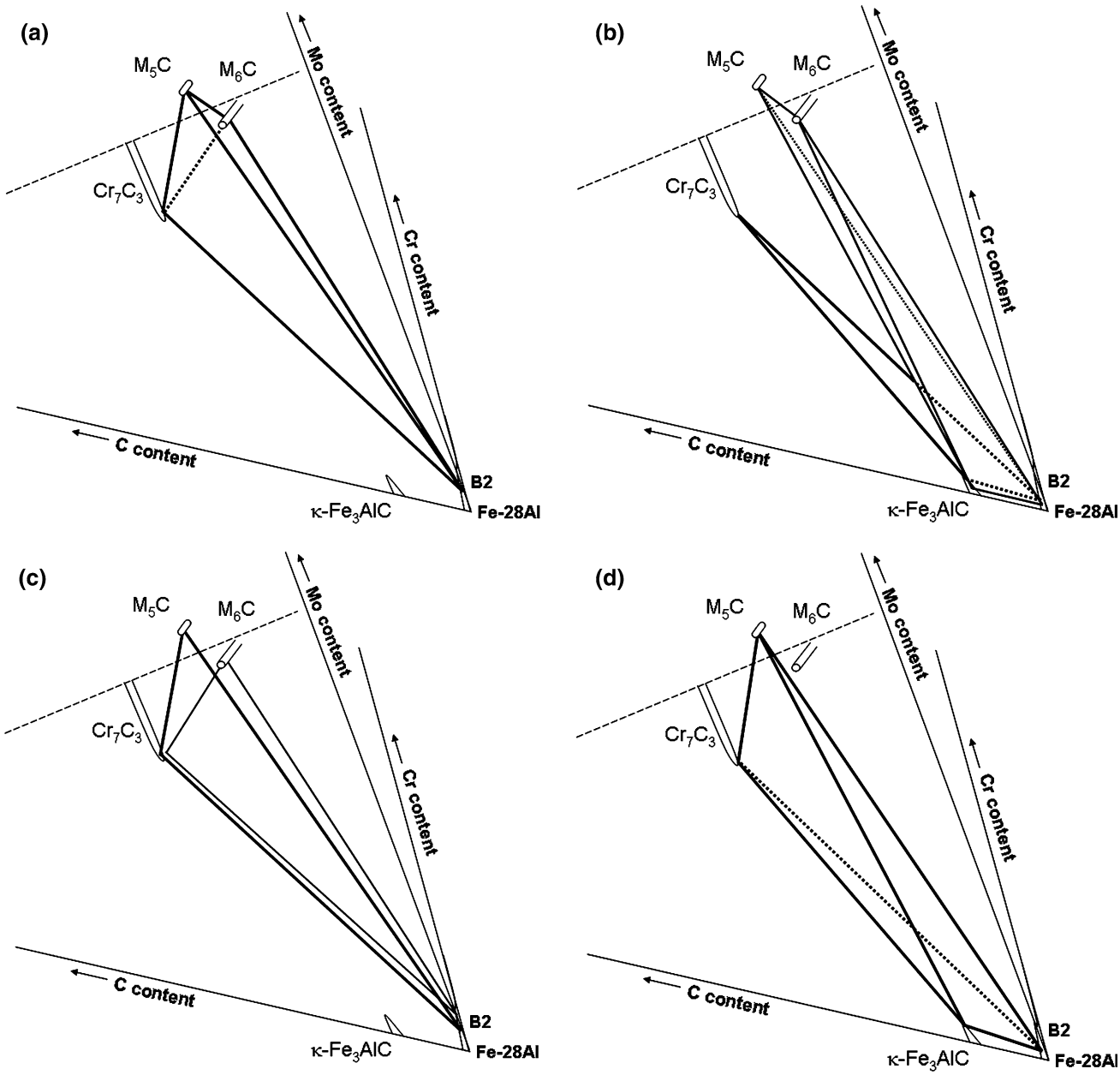

Fig. 8 The isothermal tetrahedron of the Fe_3Al-rich portion of the Fe_3Al-Cr-Mo-C pseudo-quaternary system studied by our diffusion-multiple experiments (a, b) and the conventional bulk alloy method (c, d). (a) The four-phase coexisting region of M_5C + M_6C + Cr_7C_3 + B2 in the Cr-rich composition range. (b) The three-phase coexisting region of Cr_7C_3 + κ + B2 (thicker lines) and the four-phase region of M_5C + M_6C + κ + B2 phases (thinner lines) in the Cr-poor composition range. (c) Two types of three-phase coexisting regions: M_5C + Cr_7C_3 + B2 (solid line) and M_6C + Cr_7C_3 + B2 (broken line). (d) The four-phase existing region of M_5C + Cr_7C_3 + κ-Fe_3AlC + B2

were compared with those obtained from the conventional bulk alloy method. The results obtained are as follows:

1. The following five carbide phases were formed in the Fe_3Al matrix phase (B2) with the composition gradients of Cr, Mo, and C: κ-Fe_3AlC, M_5C, M_6C, Cr_7C_3, and M_2C (M: Mo, Cr, Al, and Fe).
2. B2 phase is in equilibrium with κ, M_5C, M_6C, and Cr_7C_3 but not with M_2C phase.
3. The complex transition of phase regions with composition change was efficiently mapped with the diffusion-multiple technique, i.e. $M_6C + Cr_7C_3 + B2 \rightarrow M_5C + M_6C + Cr_7C_3 + B2 \rightarrow M_5C + M_6C + B2 \rightarrow M_5C + M_6C$ + κ-Fe_3AlC + B2 $\rightarrow M_6C$ + κ-Fe_3AlC + B2 with decreasing Cr content.
4. Phase equilibria obtained from the diffusion-multiple experiment was turned out to be consistent with the result obtained from the conventional bulk alloy method.

Table 5 The equilibrium phases and their compositions obtained from the bulk Fe_3Al-based alloys annealed at 800 °C for 1000 h

		Phase composition, at.%				
Alloy designation	**Phase present**	**Fe**	**Al**	**Cr**	**Mo**	**C**
5-1.5-1	M_6C	21.8	14	3.2	45	16
	Cr_7C_3	13.0	0.5	50.6	3.1	32.8
	Matrix	68.9	26.2	3.7	1.2	…
2-1.5-0.6	M_5C	13.8	14	7.9	46	18.3
	M_6C	21.6	14.6	2.3	46	15.5
	Matrix	70.3	27	1.8	0.9	…
2-1.2-0.6	M_5C	15	12.3	8.2	45.2	19.3
	Cr_7C_3	20	0.7	46	3	30.3
	Matrix	69.5	27.5	2.1	0.9	…
2-1-1.2	M_5C	15.5	13.5	8.4	44	18.6
	Cr_7C_3	22.4	0.7	45	2.8	29.1
	κ-Fe_3AlC	61	22.4	3.8	0.2s	12.6
	Matrix	70.2	27.7	1.5	0.6	…
0-1.2-0.6	M_6C	23.1	14.7	0	47	15.2
	κ-Fe_3AlC	66	22.9	0	0.2	10.9
	Matrix	71.6	27.8	0	0.6	…
0-1-1.2	M_6C	23.2	15.2	0	47	14.6
	κ-Fe_3AlC	65.5	22.6	0	0.2	11.7
	Matrix	71.8	27.6	0	0.6	…

5. Heat treatment time and method in the diffusion-multiple should be carefully chosen to obtain phase equilibria among all the phases in the system studied.

Acknowledgments

The authors would like to thank Mr. Kraus Markmann, Mr. Gerhard Bialkowski, Jürgen Baseler, and Ralf Selbach of the Max-Planck-Institute for Iron Research for their help with the experiments. The authors also thank Prof. JC Schuster from Institute of Physical Chemistry, University of Vienna, for helpful discussion on phase determination of carbide phases.

Open Access

References

1. J.C. Zhao, Reliability of the Diffusion-Multiple Approach for Phase Diagram Mapping, *J. Mater. Sci*, 2004, **39**, p 3913-3925
2. J.C. Zhao, M.R. Jackson, and L.A. Peluso, Determination of the Nb-Cr-Si Phase Diagram using Diffusion Multiple, *Acta Mater.*, 2003, **51**, p 6395-6405
3. S. Kobayashi and S. Zaefferer, Determination of Phase Equilibria in the Fe_3Al-Cr-Mo-C Semi-Quaternary System using a New Diffusion-Multiple Technique, *J. Alloys Compd.*, 2008, **452**, p 67-72
4. C.G. McKamey, J.H. Devan, P.F. Tortorelli, and V.K. Sikka, A Review of Recent Developments in Fe_3Al-Based Alloys, *J. Mater. Res.*, 1991, **6**, p 1779-1805
5. N.S. Stoloff, Iron Aluminides: Present Status and Future Prospects, *Mater. Sci. Eng. A*, 1998, **258**, p 1-14
6. S. Kobayashi, S. Zaefferer, A. Schneider, D. Raabe, and G. Fommeyer, Optimization of Precipitation for Controlling Recrystallisation of Wrought Fe_3Al Based Alloys, *Intermetallics*, 2005, **13**, p 1296-1303
7. S. Kobayashi and S. Zaefferer, Microstructure Control using Precipitate Phases for the Development of Heat Resistant Fe_3Al-Based Alloys, *Advanced Intermetallic-Based Alloys*, C.L. Fu, H. Clemens, J. Wiezorek, M. Takeyama, and D. Morris, Eds. (Mater. Res. Soc. Symp. Proc. 980, Warrendale, PA), 2007, p 0980-II01-03
8. S. Kobayashi and S. Zaefferer, Creation of a Fine-Grained and Deformed Structure with Fine Carbide Particles in a Fe_3Al-Cr-Mo-C Alloy, *Intermetallics*, 2006, **13**, p 1252-1256
9. M. Eumann, M. Palm, and G. Sauthoff, Alloys Based on Fe_3Al or FeAl with Strengthening Mo_3Al Precipitates, *Intermetallics*, 2004, **12**, p 625-633
10. M. Palm and G. Inden, Experimental Determination of Phase Equilibria in the Fe-Al-C System, *Intermetallics*, 1995, **3**, p 443-454
11. G. Petzow and G. Effenberg, *Ternary Alloys 8*. VCH Verlagsgesellschaft, Stuttgart, 1993, p 324-343
12. S. Zaefferer, Computer-Aided Crystallographic Analysis in the TEM, *Adv. Imag. Electron Phys.*, 2002, **125**, p 355-415
13. S. Zaefferer, New Developments of Computer-Aided Crystallographic Analysis in Transmission Electron Microscopy, *J. Appl. Crystallogr.*, 2000, **33**, p 10-25